Journal of the Serbian Chemical Society
JSCS@tmf.bg.ac.rs • www.shd.org.rs/JSCS
J. Serb. Chem. Soc. *90* (2) 187–200 (2025)
JSCS–5829
Original scientific paper
Published 20 February, 2025

Selected phytochemicals as potent acetylcholinesterase inhibitors: An *in silico* prediction

RAM LAL SWAGAT SHRESTHA[1-3], PRABHAT NEUPANE[1], SUJAN DHITAL[1], NIRMAL PARAJULI[1], BINITA MAHARJAN[1,2], TIMILA SHRESTHA[1,2], SAMJHANA BHARATI[1,2], BISHNU PRASAD MARASINI[3,4] and JHASHANATH ADHIKARI SUBIN[5]*

[1]*Department of Chemistry, Amrit Campus, Tribhuvan University, Lainchour, Kathmandu 44600, Nepal,* [2]*Kathmandu Valley College, Syuchatar Bridge, Kalanki, Kathmandu 44600, Nepal,* [3]*Institute of Natural Resources Innovation, Kalimati, Kathmandu 44600, Nepal,* [4]*Nepal Health Research Council, Ramshah Path, Kathmandu 44600, Nepal and* [5]*Bioinformatics and Cheminformatics Division, Scientific Research and Training Nepal P. Ltd., Bhaktapur 44800, Nepal*

(Received 5 April, revised 22 April, accepted 2 July 2024)

Abstract: In recent times, there has been a notable increase in the widespread presence of Alzheimer's disease. The disease could be controlled by the inhibition of acetylcholinesterase, an enzyme associated with the degradation of acetylcholine. Plants have been used to treat neurogenerative diseases and their phytochemicals could act as acetylcholinesterase inhibitors, impeding the protein's catalytic activity. This study includes a computational assessment of phytocompounds as potent inhibitors of the enzyme. The molecular docking calculations revealed binding affinities of −50.651, –49.446 , –48.400, –47.977, –47.839 and –47.417 kJ/mol for allanxanthone B, stigmasterol, 5'-*O*-methyl dioncophylline D, ismailin, wistin and dioncophylline C2, respectively, indicating firm binding of these molecules with the receptor. Donepezil (a native and FDA-approved drug) exhibited a binding affinity of –46.789 kJ/mol, which was significantly lower than that of the proposed phytochemicals. The successful candidates demonstrated good stability of the complex with the protein, showing smooth *RMSD* of ligands below 6 Å from the 200 ns molecular dynamics simulation. The thermodynamic stability from the MMPBSA method indicated the sustained spontaneity and feasibility of the adducts. Thus, the proposed candidates could be used as remedies for Alzheimer's disease after the experimental verification for their safety and efficacy.

Keywords: binding affinity; catalytic gorge; geometrical stability; free energy changes; molecular dynamics simulation.

* Corresponding author. E-mail: subinadhikari2018@gmail.com
https://doi.org/10.2298/JSC240405065S

INTRODUCTION

Alzheimer's disease (AD) is a neurological disorder resulting in a gradual and irreversible deterioration of the cognitive function.[1] It is rapidly emerging as one of the most lethal, costly and burdensome illnesses of the current era.[2] Alzheimer's disease stands as the primary contributor to dementia, a condition that ranks as the seventh most common cause of mortality.[3] Current estimates suggest that around 55 million individuals globally are suffering from it.[3]

The disease could be treated through the inhibition of acetylcholinesterase (AChE), a crucial enzyme involved in the degradation of acetylcholine by increasing the efficiency of the signal given by the brain.[4] It is a neurotransmitter and neuromodulator that binds to receptors of cells that help to contract muscle, dilate blood vessels, reduce heart rate, *etc*.[5] In the treatment of AD, the use of AChE inhibitors is intended to prevent the breakdown of acetylcholine and thus promote improvement in cholinergic neurotransmission.[4] Donepezil, rivastigmine, tacrine and galantamine are some of the promising inhibitors of the enzyme from the clinical trials.[6] The active site gorge of AChE comprises both the peripheral anionic site (PAS) and the catalytic active site (CAS, Fig. 1), which serves as the binding site for competitive inhibitors.[7] The CAS consist of SER203, GLU334 and HIS447 whereas PAS includes TYR72, ASP74, TYR124, TRP286 and TYR341 situated around the gorge of the active site. PAS has a significant role as it binds temporarily with the substrate and could block the substrate from the catalytic site.[8]

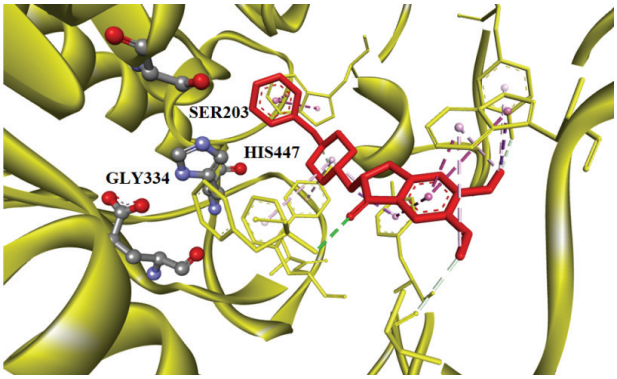

Fig. 1. Native ligand docked (red) in between the peripheral anionic site (PAS) and catalytic active site (CAS) of the protein (PBD ID: 7E3H) showing no interaction with a catalytic triad (SER203, GLY334 and HIS447).

Medicinal plants have been used in ancient Ayurvedic and folk medicines for the treatment of Alzheimer's disease.[9] Phytochemicals have been extensively explored as AChE inhibitors due to various adverse effects associated with current medications.[10] Several literatures have reported plant sources as potent inhi-

bitors of the enzyme as a means for the treatment of Alzheimer's disease.[11] Different computational approaches have been employed in the drug discovery process to facilitate experiments for cost-efficiency and enhanced effectiveness during preliminary screening.[12] Many studies have proposed phytochemicals of different medicinal plants as AChE inhibitors using computational approaches.[13] Computational drug discovery could be employed to accelerate the tedious high throughput experimental screening process by minimizing the likelihood of subsequent failures and recall during clinical trials.[14] This study incorporates *in silico* tools and techniques such as molecular docking, molecular dynamics simulation, binding free energy estimation and ADMET prediction for the exploration of potent AChE inhibitors from plant-based sources.

EXPERIMENTAL

Preparation of ligand and protein structures

A database of 77 bioactive ligands was made from the selected phytochemicals derived from African plants.[15] The 3D structure of the ligands was downloaded in sdf format from the PubChem database[16] and their molecular structures and bond order were checked using the Avogadro software.[17] The protein 3D crystalline structure with PDB ID: 7E3H[18] (X-ray resolution = 2.45 Å, expression system = *Homo sapiens*) was downloaded from the RCSB protein data bank server.[19] The protein was cleaned by removing water molecules, co-crystallized native ligand and chain B using the PyMOL program.[20] The receptor was further subjected to evaluation of geometrical structure through the ERRAT, PROCHECK and VERIFY modules of the SAVES v6.0 server.[21]

Molecular docking calculations

The DockThor server was employed for the flexible docking calculations.[22] Choice of the docking method was based on its ability to undergo multiple docking calculations within a short period of time using a freely available web server, as well as its ability to reproduce the same results.[22] The inclusion of solvated environment and protein flexibility tends to provide the best possible model to the natural system. The details of the docking parameters were adopted from recently published literature.[23] The selected parameters include the box coordinates of (–43, 36, –32), the box size of (16, 16, 16), the population size of 750, the discretization of 0.17, 24 runs and 1,000,000 evaluations. The interactions between the ligand and the amino acid residues were visualized using Biovia Discovery Studio.[24] The docking protocol was validated by achieving a root mean square deviation (*RMSD*) of less than 2 Å for the heavy atoms of the ligand, as obtained through superimposing the native ligand and the re-docked ligand (Fig. 2).

Molecular dynamics simulation (MDS) and binding free energy estimation

GROMACS program[25] was used for the simulation studies and a combination of Charmm27 force field[26] and TIP3P solvation model[27] were utilized. Other parameters were adopted from recent literature.[28] The equilibration process involved running two simulations: one under NPT conditions and another under NVT conditions, each lasting 500 ps and totalling 2 ns. These simulations were conducted at a standard body temperature of 310K. Following equilibration, a production run of 200 ns was carried out using a time step of 2 fs. Various molecular dynamics (MD) parameters were extracted from GROMACS software's built-in modules. The binding free energy post-MD simulation was determined by analysing the equilib-

rated 20 ns of the MD trajectory, employing the molecular mechanics Poisson Boltzmann solvation model.[29]

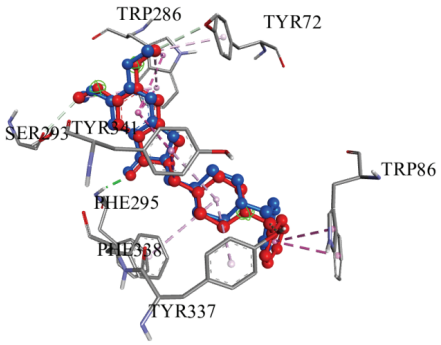

Fig. 2. Superimposition of native (red) and redocked ligand (blue) along with their interactions with amino acid residues at the catalytic pocket of protein.

The changes in binding free energy of the protein–ligand complex are given as:[28]

$$\Delta G_{BFE} = \Delta G_{complex} - \Delta G_{protein} - \Delta G_{ligand} \quad (1)$$

ADMET Prediction

The safety and drug-likeness such as toxicity, excretion, distribution, metabolism and absorption properties of the hit candidates were determined through the pkCSM server.[30]

RESULTS AND DISCUSSION

For the disruption of normal functioning of a protein through competitive inhibition, the ligand should strongly bind to the active site of the receptor protein.[31,32] The crystalline protein (PDB ID: 7E3H) contains the FDA-approved drug, donepezil[33] as a native ligand docked in between the CAS and PAS.[18] The docked ligand with stronger binding in terms of binding affinity than the native could stop the catalytic activity of the enzyme by blocking the binding to the catalytic triad.

Protein structure evaluation

The quality of protein geometry in terms of the ERRAT module was 94.21 indicating the high overall quality of the protein structure. Around 91.65 % of the amino acid residues passed the VERIFY module suggesting the good 3D structure of the protein appropriate for computational assessment. Ramachandran plots depicted that no amino acid residues were on the disallowed region out of 528 with 90 % on the most favoured region as shown in the supplementary information (Fig. S-1 of the Supplementary material to this paper).

Binding affinity from molecular docking calculation

From the molecular docking calculation, 12 compounds exhibited greater binding affinity than that of native with –46.789 kJ/mol and are shown in Tables I and S-I (Supplementary material). The best binding affinity of –50.651 kJ/mol

was observed with allanxanthrone B having a significant difference of 3.861 kJ/mol than that of donepezil. The binding affinities of –49.446, –48.400 and –48.216 kJ/mol were observed with stigmasterol, 5'-*O*-methyldioncophylline D and durallone, respectively. Other compounds like simplexin, ismailin, witsin, dioncophylline C2, asphodelin, sungucine, rotenone and azadirone also showed better binding than that of the native exceeding binding affinity of 46 kJ/mol. In addition, majority of the docked compounds showed better binding affinities than that of reference drugs, galantamine (–39.840 kJ/mol) and rivastigmine (–37.166 kJ/mol).

The stronger binding of several ligands compared to the native ligand at the orthosteric pocket of the AChE suggests their potential for superior protein inhibition.

TABLE I. Binding affinity of top candidates with protein AChE

S.N.	Ligand	PubChem CID	Binding affinity, kJ/mol
1	Allanxanthone B	11328706	–50.651
2	Stigmasterol	5280794	–49.446
3	5′-O-methyldioncophylline D	132542154	–48.400
4	Durallone	1023565	–48.216
5	Simplexin	119045	–47.990
6	Ismailin	135454728	–47.977
7	Wistin	10095770	–47.839
8	Dioncophylline C2	132500912	–47.417
9	Asphodelin	182665	–47.325
10	Sungucine	189778	–47.237
11	Rotenone	6758	–46.944
12	Azadirone	10906239	–46.814
13	Native	1150567	–46.789
14	Galantamine	9651	–39.840
15	Rivastigmine	77991	–37.166

Protein–ligand interactions

From the 2D interaction between ligand and the amino acid residues of top candidates, several interactions such as π–π stacked, alkyl, π–alkyl, π–cation, hydrogen bonds, carbon–hydrogen bonds and van der Waals were observed (Table S-II of the Supplementary material). The interactions with amino acid residues such as TRY72, TRP286, PHE295, TYR337 and TYR341 as well as one of the catalytic triad, HIS477 were observed between the docked ligand and amino acid residues of AchE (Figs. 3 and S2). The majority of interactions of the docked ligands were similar to the ones observed with the native as shown in Figs. 2 and 3 indicating that the ligands were docked at the same location as the native. Despite several electronegative centres in the majority of ligands, only a few hydrophilic interactions were detected, specifically forming hydrogen bonds

with amino acid residues ASP74, PHE295 and HIS447. In addition, one of the ligands, ismailin, showed the π–cation interaction with amino acid residue ASP74 and π–lone pair interaction with TYR124. Several van der Waals interactions with the amino acid residues of PAS and catalytic triad were observed. However, there was no observed interaction with the catalytic triad residue, GLY334, as it was positioned further away from the docked site. Similar interactions were observed in recent literature with molecular docking of AChE.[34]

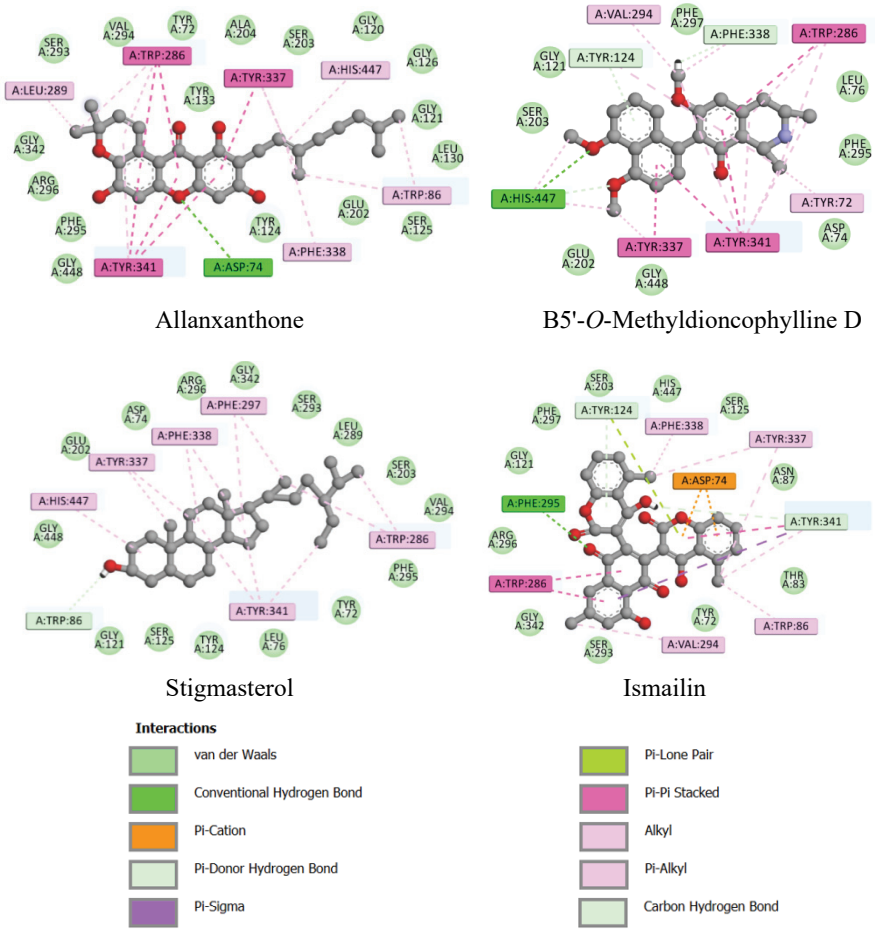

Fig. 3. 2D interaction between amino acid residues of protein (PDB ID: 7E3H) and docked ligands.

It could be deduced that the ligands were docked between the peripheral anionic site (PAS) and catalytic active site (CAS), similar to that of the native

ligand, donepezil.[7] Thus, the docked ligand could block competitive ligands reaching the catalytic triad halting the catalytic function of the receptor.

*Root mean square deviation (*RMSD*)*

RMSD of protein backbone and ligands, both with respect to the protein backbone, helps to determine the geometrical stability of the ligand with the receptor protein.[23] The deviation of ligands within the orthosteric pocket could be monitored from the *RMSD* plots shown in Fig. 4A. The plots depicted no significant deviation of the ligand from the docked pose with few trivial spikes in the *RMSD* trajectory. Dioncophylline C2, wistin, ismailin, stigmasterol, allanxanthrone B and 5'-*O*-methyldioncophylline D exhibited good stability with the enzyme having heavy atom *RMSD* of ligand below 6 Å. Dioncophylline demonstrated the best stability with a smooth trajectory and *RMSD* at around 3 Å. Stigmasterol, ismailin and wistin also exhibited good geometrical stability, with *RMSD* below 4 Å, albeit with occasional spikes in the trajectory. Despite the rise of *RMSD* of allanxanthrone B at the beginning, the system attained equilibrium after *ca.* 100 ns and smooth *RMSD* was observed up to 200 ns. In the case of 5'--*O*-methyldioncophylline D, a comparative smooth trajectory with *RMSD* of ligand at approximately 5 Å was observed. Slightly unstable nature of curve with multiple bumps and higher *RMSD* was observed in case of durallone and simplexin as depicted in Fig. S-3 of the Supplementary material. The protein backbone *RMSD* remained steady and smooth at around 2 Å (Fig. 4B) without noticeable bumps or spikes inferring the stability of protein structure upon ligand binding.

From the *RMSD* trajectory, it could be deduced that the ligand attained geometrical stability within the orthosteric pocket of AChE without significant deviation in terms of the *RMSD* of the ligand.

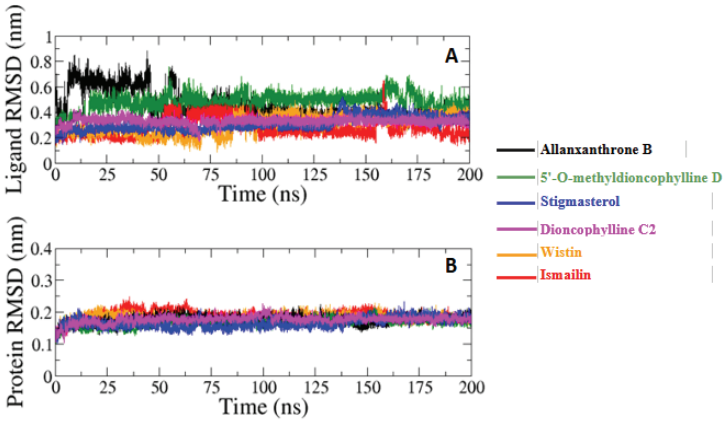

Fig. 4. *RMSD* of ligands (A) and protein (B) of dioncophylline C2 (magenta), wistin (orange), ismailin (red), stigmasterol (blue), allanxanthrone B (dark) and 5'-*O*-methyldioncophylline D (green) complexes.

The relative rotational and translation motion of the ligands could be monitored from the snapshots retrieved at different times from the molecular dynamics simulation.[23,28] From the snapshots (Fig. S-4 of the Supplementary material) it was evident that the ligand remained in its docked location between the PAS and CAS with minute alteration of position and orientation. Despite lower translational motion, a significant rotational motion could be observed for the majority of ligands which were reflected by a few spikes and bumps in the *RMSD* profiles. The shift of position of witsin could have contributed to sudden spikes in the *RMSD* curve. The *RMSD* curve of the ligand of allanxanthrone B complex and the relative position of the ligand at the docked site were correlated as the ligand underwent significant rotation and was localized after the attainment of equilibrium as depicted in Fig. 4. In spite of a noticeable rotational shift, the docked ligands remained localized within the orthosteric pocket and thus could result in inhibition of the AChE enzyme.

The radial-distribution curve depicts the presence of a single sharp peak for dioncophylline C2, wistin and stigmasterol inferring the localization of ligands without any change in center of mass[35] as shown in Fig. 5. However, ismailin, allanxanthrone B and 5'-*O*-methyldioncophylline D demonstrated two peaks, one large peak and another small ridge signifying that the ligand's centre of mass shifted between the two, with a predominant presence at one particular site.

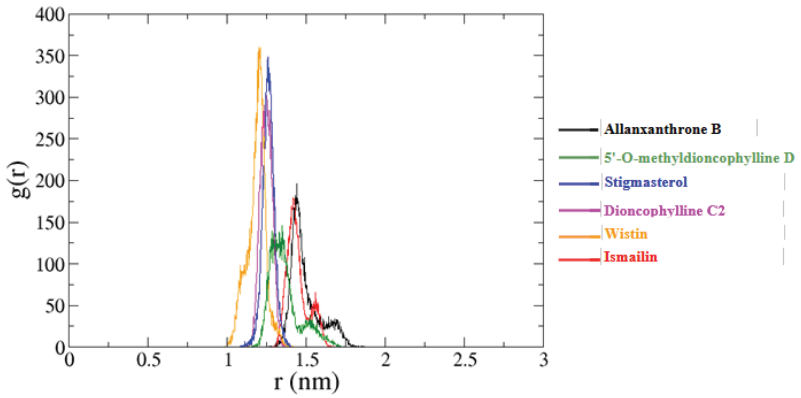

Fig. 5. Radial pair distribution function ($g(r)$) of the ligands' centre of mass with reference to that of the protein in dioncophylline C2 (magenta), wistin (orange), ismailin (red), stigmasterol (blue), allanxanthrone B (dark) and 5'-*O*-methyldioncophylline D (green) complexes.

*Other geometrical evaluators (*RMSF, R_g, SASA *and H-bond)*

The root mean square fluctuation (*RMSF*) plot of the protein backbone (α--carbon) is depicted in Fig. 6. *RMSF* plot helps to evaluate the stability of the protein structure as an unstable loop structure shows greater fluctuation as com-

pared to stable sheet and helix structures.[36] The fluctuation of amino acid residues was less than 2 Å with an exception at *ca.*76 and 430 amino acid residue numbers. The amino acid residues of PAS and the catalytic triad were not in the proximity of the spiked region, demonstrating a fluctuation less than approximately 1.5 Å. Among the catalytic triad, GLU334 showed slightly higher fluctuation than SER203 and HIS447. This might be attributed to the binding of the docked ligand with SER203 and HIS447 only. The amino acids interacting with the docked ligands such as TRP72, ASP74, TRY124, TRP286 and TYR341 demonstrated lesser fluctuations as compared to other amino acid residues which might be due to induced stability from stronger binding with the docked ligands.

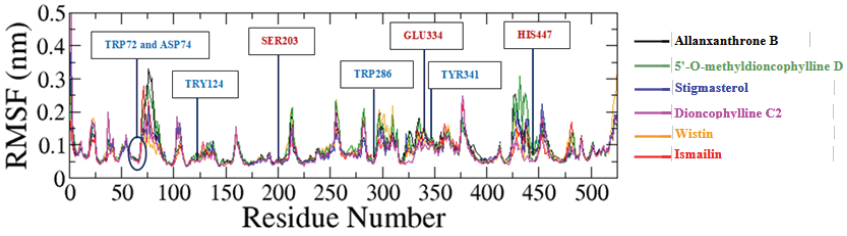

Fig. 6. *RMSF* plot of protein backbone of dioncophylline C2 (magenta), wistin (orange), ismailin (red), stigmasterol (blue), allanxanthrone B (black) and 5'-O-methyldioncophylline D (green) complexes.

The solvent-accessible surface area (*SASA*) of all the complexes were nearly the same at approximately 215±10 nm^2 inferring the stability of protein structure upon the interaction with the ligands[37] as depicted in Fig. 7. The *SASA* trajectory remained smooth without any significant bumps and spikes indicating that the hydrophobic region of the receptor was not exposed upon ligand binding. A similar smooth trajectory was seen in the case of the radius of gyration (R_g) of complexes at *ca.* 23±0.25 Å, signifying no change in protein conformation in terms of expansion and contraction.[38] The steady and smooth trajectory of R_g and *SASA* retrieved from the MDS trajectory emphasized the geometrical stability of the protein structure upon ligand binding.

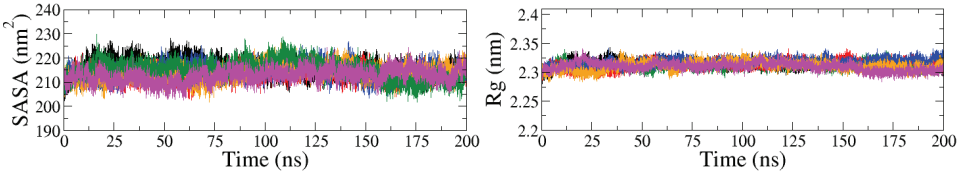

Fig. 7. *SASA* (left) and R_g (right) of protein of dioncophylline C2 (magenta), wistin (orange), ismailin (red), stigmasterol (blue), allanxanthrone B (dark) and 5'-*O*-methyldioncophylline D (green) complexes.

The hydrogen bonds formed between the amino acid residues throughout the 200 ns production run was monitored since hydrogen bond governs several biological processes such as metabolism, adsorption, drug affinity and specificity.[39] From the MD simulation, a noticeable variation in the number of hydrogen bond formation of each complex could be observed as shown in Fig. 8. Allanxanthrone B, stigmasterol, 5'-*O*-methyldioncophylline D and dioncophylline C2 demonstrated almost similar number of hydrogen bond formation around 2 to 4. A significant contrast could be observed in case of wistin and ismailin. Wistin demonstrated a maximum number of hydrogen bond formations with 7 to 8, whereas, the lowest hydrogen bond count was seen in isamailin complex.

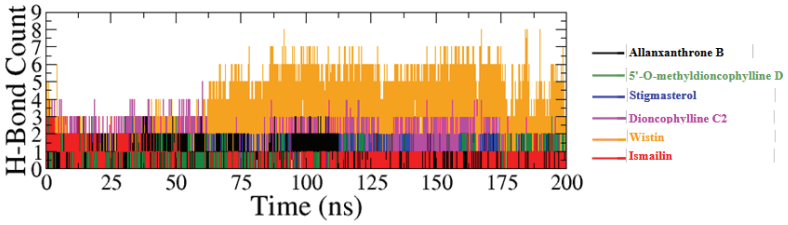

Fig. 8. Number of hydrogen bonds formed between the amino acid residues and dioncophylline C2 (magenta), wistin (orange), ismailin (red), stigmasterol (blue), allanxanthrone B (dark) and 5'-*O*-methyldioncophylline D (green).

Binding free energy change estimation (ΔG$_{BFE}$)

The change in binding free energy of the adducts from the MMPBSA method was used to assess the spontaneity and feasibility of the reaction as shown in Table II. A higher negative binding free energy (ΔG_{BFE}) indicates higher spontaneity and feasibility of the reaction.[40] The best binding free energy change was observed with stigmasterol with –131.33±18.24 kJ/mol. Binding free energy change of –108.36±18.66, –94.60±19.49, –93.59±29.32, –89.99±18.49 and –77.61±17.07 kJ/mol was observed with dioncophylline C2, allanxanthone B, wistin, 5′-*O*-methyldioncophylline D and ismailin, respectively. Except for the highest and the lowest scorers, all other complexes showed nearly identical changes in binding free energy. Among the several components, the change in energy due to van der Waals force of interaction was significant compared to

TABLE II. Change in binding free energy (kJ/mol) of hit candidates

Complex	ΔG_{BFE}
Allanxanthone B	–94.64±19.49
Stigmasterol	–131.33±18.24
5′-*O*-Methyldioncophylline D	–89.99±18.49
Ismailin	–77.61±17.07
Wistin	–93.59±29.32
Dioncophylline C2	–108.36±18.66

others. This outcome could be due to the cumulative contribution of several van der Waals interactions as shown in 2D protein–ligand interactions (Fig. 3 and Table S-III of the Supplementary material). All the complexes exhibited negative ΔG_{BFE} indicating thermodynamically stable complexes with sustained spontaneity.

Drug-likeness and safety

The comparative prediction of ADMET properties of the successful candidates, native and reference drug compounds is shown in Tables S-IV and S-V of the Supplementary material. From the comparative analysis, it was found that wistin and stigmasterol showed moderate to good drug-likeness properties with almost no toxicity. These results were better than that of other successful candidates and comparable with the native and the two reference drugs. However, *in vivo* and *in vitro* experiments should still be performed to ascertain these predictions.

CONCLUSION

The *in silico* approach revealed the phytochemicals such as dioncophylline C2, wistin, ismailin, stigmasterol, allanxanthrone B and 5'-*O*-methyldioncophylline D as potent inhibitors of the acetylcholinesterase enzyme. The compounds showed good geometrical and thermodynamical stability with the protein and could inhibit the enzyme by preventing its catalytic functions. However, several *in vitro* and *in vivo* experiments need to be done to evaluate their safety and effectiveness. Therefore, plant-based compounds could be applied in the treatment of neurodegenerative diseases like Alzheimer's.

SUPPLEMENTARY MATERIAL

Additional data and information are available electronically at the pages of journal website: https://www.shd-pub.org.rs/index.php/JSCS/article/view/12876, or from the corresponding author on request.

ИЗВОД

ОДАБРАНЕ ФИТОХЕМИКАЛИЈЕ КАО МОЋНИ ИНХИБИТОРИ АЦЕТИЛХОЛИНЕСТЕРАЗА: *IN SILICO* ПРЕДВИЂАЊЕ

RAM LAL SWAGAT SHRESTHA[1-3], PRABHAT NEUPANE[1], SUJAN DHITAL[1], NIRMAL PARAJULI[1], BINITA MAHARJAN[1,2], TIMILA SHRESTHA[1,2], SAMJHANA BHARATI[1,2], BISHNU PRASAD MARASINI[3,4] и JHASHANATH ADHIKARI SUBIN[5]

[1]Department of Chemistry, Amrit Campus, Tribhuvan University, Lainchour, Kathmandu 44600, Nepal, [2]Kathmandu Valley College, Syuchatar Bridge, Kalanki, Kathmandu 44600, Nepal, [3]Institute of Natural Resources Innovation, Kalimati, Kathmandu 44600, Nepal, [4]Nepal Health Research Council, Ramshah Path, Kathmandu 44600, Nepal и [5]Bioinformatics and Cheminformatics Division, Scientific Research and Training Nepal P. Ltd., Bhaktapur 44800, Nepal

У скорије време је дошло до приметног распрострањивања Алцхајмерове болести. Болест се може контролисати инхибицијом ацетилхолинестеразе, ензима повезаног са деградацијом ацетилхолина. Биљке које су коришћене за лечење неурогенеративних

болести и њихове фитохемикалије могу деловати као инхибитори ацетилхолинестеразе, спречавајући каталитичку активност протеина. Ова студија садржи рачунарску процену фитојединења као моћних инхибитора ензима. Израчунавања молекулског докинга показују афинитете везивања од –50,651, –49,446, –48,400, –47,977, –47,839 и –47,417 kJ/mol за алаксантон B, стигмастерол, 5'-O-метил дионкофилин D, исмаилин, вистин, односно дионкофилин C2, што указује на чврсто везивање ових молекула за рецептор. Донезепил (нативни и од FDA одобрен лек) испољава везивни афинитет од –46,789 kJ/mol, који је знатно нижи него код предложених фитохемикалија. Успешни кандидати су показали добру стабилност комплекса са протеином, показујући глатку *RMSD* лиганада испод 6 Å из симулације молекулске динамике током 200 ns. Термодинамичка стабилност по MM-PBSA методи указује на сталну спонтаност и остварљивост адуката. Тако се предложени успешни кандидати могу користити као лекови за Алцхајмерову болест након експерименталне провере њихове безбедности и ефикасности.

(Примљено 5. априла, ревидирано 22. априла, прихваћено 2. јула 2024)

REFERENCES

1. B. Ibach, E. Haen, H. E. Klein, *Curr. Pharm. Des.* **10** (2004) 231 (https://doi.org/10.2174/1381612043386509)
2. P. Scheltens, B. D. Strooper, M. Kivipelto, H. Holstege, G. Chételat, C. E. Teunissen, J. Cummings, W. M. van der Flier, *Lancet* **397** (2021) 1577 (https://doi.org/10.1016/S0140-6736(20)32205–4)
3. World Health Organization (WHO), https://www.who.int/news-room/fact-sheets/detail/dementia (3 March 2024)
4. V. N. Talesa, *Mech. Ageing Dev.* **122** (2001) 1961 (https://doi.org/10.1016/S0047-6374(01)00309-8)
5. M. R. Picciotto, M. J. Higley, Y. S. Mineur, *Neuron* **76** (2012) 116 (https://doi.org/10.1016/j.neuron.2012.08.036)
6. M. Racchi, M. Mazzucchelli, E. Porrello, C. Lanni, S. Govoni, *Pharmacol. Res.* **50** (2004) 441 (https://doi.org/10.1016/j.phrs.2003.12.027)
7. D. A. Belinskaia, P. A. Voronina, D. V. Krivorotov, R. O. Jenkins, N. V. Goncharov, *Pharmaceutics* **15** (2023) 2159 (https://doi.org/10.3390/pharmaceutics15082159)
8. G. Johnson, S. W. Moore, *Curr. Pharm. Des* **12** (2006) 217 (https://doi.org/10.2174/138161206775193127)
9. T. Dubey, S. Chinnathambi, *Arch. Biochem. Biophys.* **676** (2019) 108153 (https://doi.org/10.1016/j.abb.2019.108153)
10. H. Khan, Marya, S. Amin, M. A. Kamal, S. Patel, *Biomed. Pharmacother.* **101** (2018) 860 (https://doi.org/10.1016/j.biopha.2018.03.007)
11. N. A. Masondo, G. I. Stafford, A. O. Aremu, N. P. Makunga, *South African J. Bot.* **120** (2019) 39 (https://doi.org/10.1016/j.sajb.2018.09.011)
12. C. L. Hung, C. C. Chen, *Drug Dev. Res.* **75** (2014) 412 (https://doi.org/10.1002/ddr.21222)
13. B. Sarkar, S. Alam, T. K. Rajib, S. S. Islam, Y. Araf, M. A. Ullah, *Egypt. J. Med. Hum. Genet.* **22** (2021) 10 (https://doi.org/10.1186/s43042-020-00127-8)
14. S. S. Ou-Yang, J. Y. Lu, X. Q. Kong, Z. J. Liang, C. Luo, H. Jiang, *Acta Pharmacol. Sin.* **33** (2012) 1131 (https://doi.org/10.1038/aps.2012.109)
15. B. D. Bekono, F. Ntie-Kang, P. A. Onguéné, L. L. Lifongo, W. Sippl, K. Fester, L. C. O. Owono, *Malar. J.* **19** (2020) 183 (https://doi.org/10.1186/s12936-020-03231-7)

16. S. Kim, J. Chen, T. Cheng, A. Gindulyte, J. He, S. He, Q. Li, B. A. Shoemaker, P. A. Thiessen, B. Yu, L. Zaslavsky, J. Zhang, E. E. Bolton, *Nucleic Acids Res.* **51** (2023) D1373 (https://doi.org/10.1093/nar/gkac956)
17. M. D. Hanwell, D. E. Curtis, D. C. Lonie, T. Vandermeerschd, E. Zurek, G. R. Hutchison, *J. Cheminform.* **4** (2012) 17 (https://doi.org/10.1186/1758-2946–4-17)
18. K. V. Dileep, K. Ihara, C. Mishima-Tsumagari, M. Kukimoto-Niino, M. Yonemochi, K. Hanada, M. Shirouzu, K. Y. J. Zhang, *Int. J. Biol. Macromol.* **210** (2022) 172 (https://doi.org/10.1016/j.ijbiomac.2022.05.009)
19. H. M. Berman, J. Westbrook, Z. Feng, G. Gilliland, T. N. Bhat, H. Weissig, I. N. Shindyalov, P. E. Bourne, *Nucleic Acids Res.* **28** (2000) 235 (https://doi.org/10.1093/nar/28.1.235)
20. S. Yuan, H. C. S. Chan, Z. Hu, *WIREs Comp. Mol. Sci.* **7** (2017) e1298 (https://doi.org/10.1002/wcms.1298)
21. C. Colovos, T. O. Yeates, *Protein Sci.* **2** (1993) 1511 (https://doi.org/10.1002/pro.5560020916)
22. K. B. Santos, I. A. Guedes, A. L. M. Karl, L. E. Dardenne, *J. Chem. Inf. Model.* **60** (2020) 667 (https://doi.org/10.1021/acs.jcim.9b00905)
23. R. L. S. Shrestha, B. Maharjan, T. Shrestha, B. P. Marasini, J. Adhikari Subin, *Results Chem.* **7** (2024) 101363 (https://doi.org/10.1016/j.rechem.2024.101363)
24. U. Baroroh, M. Biotek, Z. S. Muscifa, W. Destiarani, F. G. Rohmatullah, M. Yusuf, *Indones. J. Comput. Biol.* **2** (2023) 22 (https://doi.org/10.24198/ijcb.v2i1.46322)
25. M. J. Abraham, T. Murtola, R. Schulz, S. Páll, J. C. Smith, B. Hess, E. Lindah, *SoftwareX* **1** (2015) 19 (https://doi.org/10.1016/j.softx.2015.06.001)
26. V. Zoete, M. A. Cuendet, A. Grosdidier, O. Michielin, *J. Comput. Chem.* **32** (2011) 2359 (https://doi.org/10.1002/jcc.21816)
27. W. L. Jorgensen, J. Chandrasekhar, J. D. Madura, R. W. Impey, M. L. Klein, *J. Chem. Phys.* **79** (1983) 926 (https://doi.org/10.1063/1.445869)
28. P. Neupane, J. Adhikari Subin, R. Adhikari, *J. Biomol. Struct. Dyn.* (2024) 1 (https://doi.org/10.1080/07391102.2024.2314262)
29. M. S. Valdés-Tresanco, M. E. Valdés-Tresanco, P. A. Valiente, E. Moreno, *J. Chem. Theory Comput.* **17** (2021) 6281 (https://doi.org/10.1021/acs.jctc.1c00645)
30. D. E. Pires, T. L. Blundell, D. B. Ascher, *J. Med. Chem*. **58** (2015) 4066 (https://doi.org/10.1021/acs.jmedchem.5b00104)
31. R. L. S. Shrestha, R. Panta, B. Maharjan, T. Shrestha, S. Bharati, S. Dhital, P. Neupane, N. Parajuli, B. P. Marasini, J. Adhikari Subin, *Mor. J. Chem* **12** (2024) 776 (https://doi.org/10.48317/IMIST.PRSM/morjchem-v12i2.46845)
32. P. Neupane, S. Dhital, N. Parajuli, T. Shrestha, S. Bharati, B. Maharjan, J. Adhikari Subin, R. L. S. Shrestha, *J. Nepal Phys. Soc.* **9** (2023) 95 (https://doi.org/10.3126/jnphyssoc.v9i2.62410)
33. E. Y. Shintani, K. M. Uchida, *Am. J. Health-Syst. Pharm.* **54** (1997) 2805 (https://doi.org/10.1093/ajhp/54.24.2805)
34. Q. M. S. Jamal, M. I. Khan, A. H. Alharbi, V. Ahmad, B. S. Yadav, *Nutrients* **15** (2023) 1579 (https://doi.org/10.3390/nu15071579)
35. T. R. Lamichhane, M. P. Ghimire, *Heliyon* **7** (2021) E08220 (https://doi.org/10.1016/j.heliyon.2021.e08220)
36. B. K. Raut, S. R. Upadhyaya, J. Bashyal, N. Parajuli, *ACS Omega* **8** (2023) 43617 (https://doi.org/10.1021/acsomega.3c05082)

37. E. Durham, B. Dorr, N. Woetzel, R. Staritzbichler, J. Meiler, *J. Mol. Model.* **15** (2009) 1093 (https://doi.org/10.1007/s00894-009-0454-9)
38. M. Y. Lobanov, N. S. Bogatyreva, O. V. Galzitskaya, *Mol. Biol.* **42** (2008) 623 (https://doi.org/10.1134/S0026893308040195)
39. A. Shrestha, S. R. Upadhyaya, B. K. Raut, S. Bhattarai, K. R. Sharma, N. Parajuli, J. K. Sohng, & B. P. Regmi, *Processes* **12** (2024) 230 (https://doi.org/10.3390/pr12010230)
40. Z. Cournia, B. Allen, W. Sherman, *J. Chem. Inf. Model.* **57** (2017) 2911 (https://doi.org/10.1021/acs.jcim.7b00564).